

# CHARACTERIZATION OF CRACKING IN STRAIN HARDENING CEMENTITIOUS COMPOSITES USING THE COMPACT TENSION TEST

Eduardo B. Pereira<sup>\*</sup>, Gregor Fischer<sup>†</sup> and Joaquim A. O. Barros<sup>\*</sup>

<sup>\*</sup> ISISE, Dep. Civil Eng., School Eng., University of Minho  
Campus de Azurém 4800-058 Guimarães, Portugal  
e-mail: eduardo.pereira@civil.uminho.pt, barros@civil.uminho.pt, web page: www.isise.net

<sup>†</sup> Dep. Civil Eng., Technical University of Denmark  
Brovej, bygn. 118, DK-2800 Kgs. Lyngby, Denmark  
e-mail: gf@byg.dtu.dk, web page: www.dtu.dk

**Keywords:** Tension, crack, composite, fibers, design.

**Summary:** *The characterization of the tensile behavior of strain hardening cementitious composites (SHCC) is of significant importance to the material design. In a previous work the tensile stress-crack opening response of different types of SHCC was characterized using notched specimens tested in direct tension, where a single crack was obtained and mechanically characterized by performing Single Crack Tension Test (SCTT). In this study the tensile behavior of SHCC materials is characterized under eccentric tensile load using the Compact Tension Test (CTT). The long edge notch placed in the rectangular plate specimens and the eccentrically applied tensile load create the local conditions necessary to the initiation of a single crack at the tip of the notch. Further propagation and opening of the crack in Mode I allow the assessment of the tensile load-displacement relationship. The experimental results are discussed and compared to the numerically derived responses. The tensile load-displacement responses observed in the CTTs were simulated using the cohesive crack model. The tensile stress-crack opening behaviors previously obtained with the SCTT tests were utilized to derive the traction-separation laws assigned to the interface elements. The results obtained with the CTT are analyzed and discussed, with special emphasis on the possibility of using the SCTT responses to predict the structural behavior of SHCC.*

## 1 INTRODUCTION

The technological development of a wide variety of fibers in recent years has been creating new opportunities to improve the mechanical properties of Strain Hardening Cementitious Composites (SHCC) as a structural material. SHCC design nowadays aims at the development of materials with exceptional energy dissipation ability and extreme tensile performance. The intention is to mitigate the limitations of conventional concrete deriving from its quasi-brittle nature, often revealed by the catastrophic collapse of structures during extreme loading events or the early loss of functional properties of structures due to insufficient durability.

In the past few decades the research carried out in the field of fiber reinforced cementitious composites has suggested different approaches to the design of these materials [1]. In particular, when fiber reinforced cementitious composites are designed to develop strain-hardening and multiple cracking in tension occurs, SHCC materials are obtained. The design of these materials is driven by different motivations, mainly the optimization of the tensile strength or the tensile ductility. Typically, when one of these properties is enhanced by design, the other is somehow sacrificed. Engineered Cementitious Composites (ECC), a class of cement based materials typically reinforced with Polyvinyl Alcohol (PVA) fibers, is one example of SHCC designed with a special focus on tensile ductility, with relatively high tensile strain hardening ability (between 3% and 7% of ultimate tensile strain) and average tensile strength of 5 MPa [2].

The mechanical behavior of SHCC is the result of a delicate balance of multiple factors. The interfacial

bonding and fiber pull-out properties, the material parameters of the fibers and of the matrix, the distribution of material flaw sizes in the matrix, the fiber orientation and their dispersion in the matrix play an important role in the resulting composite mechanical behavior. The study of the influence of all these parameters separately is difficult, since they perform in a highly coupled manner. At a smaller scale, the fiber pull-out tests are often carried out to study the interaction between the single fiber and the matrix. Although this information is of significant importance, the reliability and objectiveness of the results obtained is often questioned mainly because the mechanical behavior exhibited by the isolated fiber while being pulled out is seldom comparable to the mechanics of the same fiber embedded in the SHCC. The type of test most commonly used, either to characterize or to design SHCC, is the direct tension test using dumbbell-shaped or coupon specimens [3,4]. The material tensile stress-strain behavior is thereby assessed, as well as the potential of the material to develop multiple cracks. Although with additional uncertainty, inverse analysis is often alternatively used to derive indirectly the tensile stress-separation law from bending or diametric compression tests, like the Compact Tension Test (CT), the Wedge Splitting Test (WST), the Four Point Bending Test and the Brazilian Compression test among others (see for example [5]).

The assessment of the tensile behavior of SHCC in terms of the stress-crack opening response is often regarded as the most suitable approach to evaluate the tensile performance of SHCC. The main obstacle to this strategy is the difficulty associated with the initiation and propagation of a single crack when the material is especially designed to develop multiple cracks. In order to produce the adequate mechanical conditions for the initiation and evolution of a single crack, the stress fields generated on test specimens under tension need to be locally intensified. This may be achieved by introducing constrictions or notches at predetermined sections [5-7]. This procedure is extensively used to characterize the tensile response of tensile softening fiber reinforced cementitious composites. In the present work the single crack tension test (SCTT) setup was used to assess the tensile stress-crack opening response of three different SHCC. Although the formation of a single crack during testing was confirmed in previous studies [9], further investigation is required to confirm the applicability of the derived tensile stress-crack opening responses to objectively characterize the constitutive tensile behavior of these materials. In this research the tensile stress-crack opening responses of three different fiber reinforced cementitious composites are used to predict the load-deformation responses obtained with a different type of test, in this case the compact tension test (CTT). The results obtained with a numerical model constructed to simulate the CTT are compared with the experimental responses.

## **1.2 Digital image analysis of cracking process**

The understanding of the micro-cracking mechanisms taking place near the tip of propagating cracks is relevant for the optimal design of SHCC. The research described in the literature towards the better understanding of the fracture process zone in cement-based matrix composites reports the development of special techniques to analyze cracking. The very fine cracks to be detected require high resolution equipments [10,12]. In addition, most of the intrusive characterization techniques used in other materials potentially induce preliminary cracks in concrete, either due to direct mechanical action, induced drying, or the alteration of other physical variables important for the delicate balance of the microstructure of concrete. Many different techniques have been especially developed to the analysis of the fracture process zone and cracking in concrete and other cement based materials. Radiography (x-rays, neutrons, or others), dye impregnation, acoustic emission, ultrasound, laser holography and interferometry are examples of techniques utilized in the past to obtain quantitative information about the fracture process zone [11-14]. Although most of the macroscopic features of cracking process in concrete are well understood, the micro-mechanisms of cracking and the essence of the fracture process zone are still uncertain.

Recent developments in digital photography technology have reached significant improvements in the quality of digital acquisition of images for scientific research. In particular, the digital image correlation technique has been developed, which allows the derivation of the full field surface displacements and strains of objects under load, based on the comparison of two digitized images of the surface of an object before and after deformation [15]. In this study the cracking behavior of the tested cementitious composites was

investigated. The purpose was to identify the important features of the cracking process at the surface of the specimen, and use this information to support the interpretation and discussion of the CTT mechanical results obtained.

## 2 MATERIALS

In this research the tensile behavior of three different fiber reinforced cementitious composites was investigated. Both the type of fiber reinforcement and the composition of the matrix were different in the composites tested. Fibers of three different natures were used: PVA (polyvinyl alcohol), PAN (polyacrylonitrile) and PP (polypropylene). The main properties of the fibers used are presented in Table 1.

Table 1 : Main properties of the fibers.

Fiber	Tensile strength	Length	Diameter
	MPa	mm	$\mu\text{m}$
PVA	1600	8	40.0
PP	900	12	40.0
PAN 1.5	826	6	12.7

The composition of each fiber reinforced cementitious composite is represented in Table 2. As shown two different types of cementitious matrices were used. The volume fraction of fiber reinforcement employed was 2% in the case of the PVA (PVAcc) and the PAN (PANcc) fiber reinforced cementitious composites, and 2.5% in the case of the PP fiber reinforced cementitious composite (PPcc). The higher volume fraction in the case of the PPcc aimed at compensating the lower tensile strength of PP fibers when compared to the PVA ones. In the case of the PANcc this compensation was not considered due to the significant influence of the fiber volume increase in the flow properties of the fresh mix.

Table 2: Weight proportions of the materials used in each composite.

Composite	Fiber reinforcement	Cement	Fly ash	Fine sand (0.17 mm)	Quartz powder	Water
PVAcc	2% PVA	1	2	0.35	0.35	0.75
PPcc	2.5% PP	1	2	0.35	0.35	0.75
PANcc	2% PAN	1	6	0	0	1.40

## COMPACT TENSION TEST (CTT)

### 2.1 Testing procedure

The CTT testing procedure consisted on applying an eccentric tensile load to a single-edge notched specimen, at a constant displacement rate of  $5 \mu\text{m/s}$ , to induce the initiation of a single crack and allow its propagation in a controlled manner. The dimensions and geometry of the specimen are presented in Figure 1. The thickness of the specimen was minimized to 12 mm, promoting the plane stress condition in the loaded specimen. Further details about the testing procedure may be found elsewhere [16].

The formation and propagation of the tensile crack was traced on the surface of the specimens using a

high resolution digital camera, positioned 90 mm away from the specimen. The 60 mm focal length lens allowed the observation of a 24 mm by 36 mm area of the surface of the specimen (see Figure 2). Images with 24 megapixel of resolution were captured during testing with time intervals of one second. These images were subsequently used to continuously interpolate the strain fields at the inspected surface of the specimen.

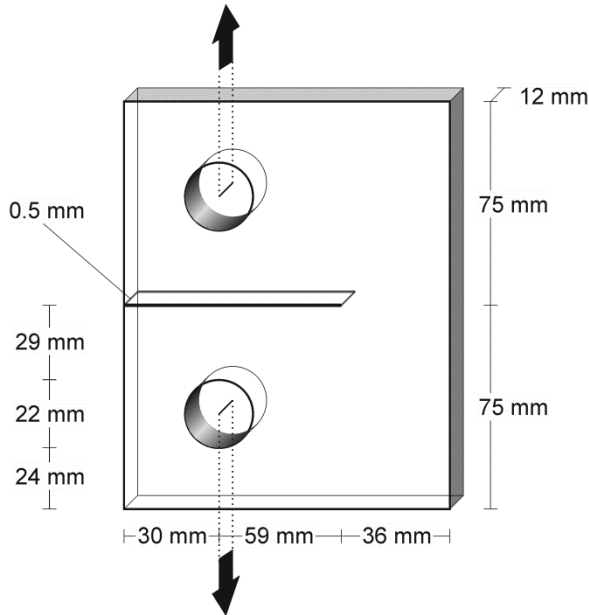


Figure 1: Geometry and dimensions of the CTT specimen.

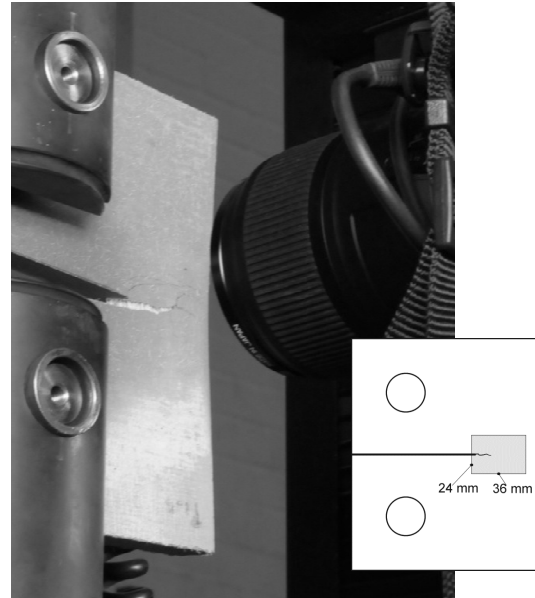


Figure 2: Image of test-setup and size of the documented area.

The optimal conditions to the strain field interpolation were met without the need of applying a speckle pattern on the surface of the specimen, in contrast with the typical procedure when applying this technique. Sufficient randomness and high contrast of the stochastic patterns captured from the surface are important to the continuous recognition and tracing of the shape and position of each facet [17]. The images of the surface of the specimens were analyzed prior to testing and sufficient image correlation was obtained. Each facet was composed of  $15 \times 15$  pixels. Each pixel covered a real area of  $6 \times 6 \mu\text{m}^2$ . The total area of  $24 \times 36 \text{ mm}^2$  was modeled by a facet mesh overlay composed of approximately  $267 \times 400$  facets.

## 2.2 Load – displacement results

The experimental responses obtained for the three composites in terms of the tensile load *versus* the displacement are presented in Figure 3 to Figure 5. For comparison, in Figure 6 the average responses of each composite are presented. The average responses were obtained by averaging the tensile load values measured for the three specimens of each composite at every displacement level.

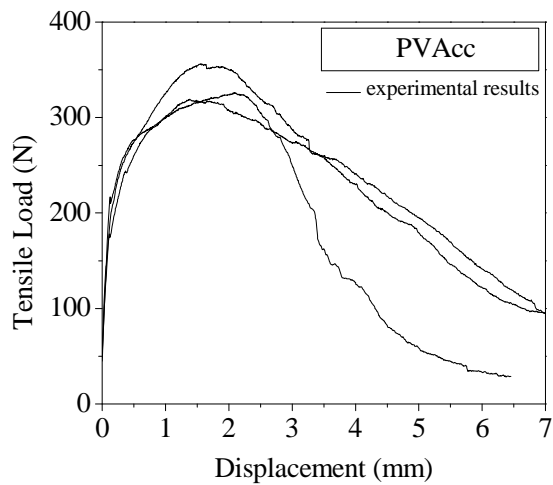


Figure 3: Tensile load – displacement for the composites reinforced with PVA fibers.

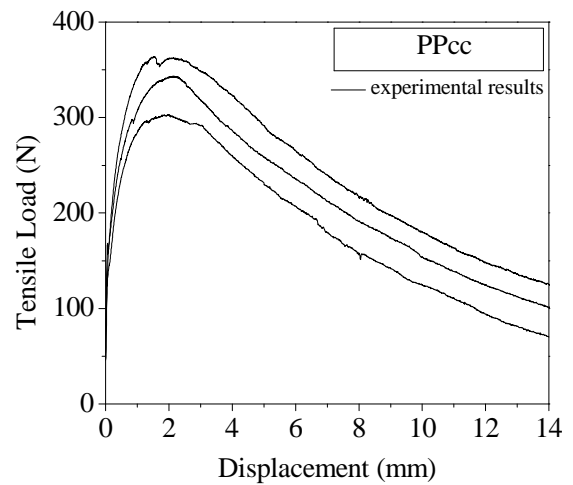


Figure 4: Tensile load – displacement for the composites reinforced with PP fibers.

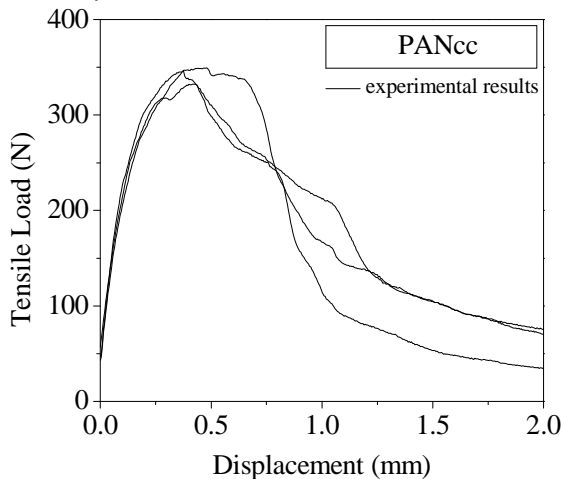


Figure 5: Tensile load – displacement for the composites reinforced with PAN fibers.

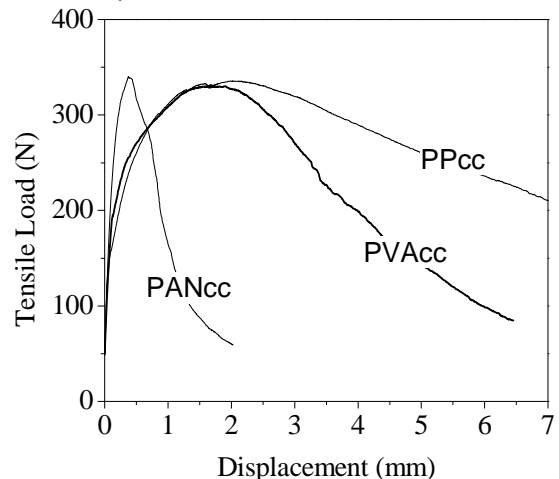


Figure 6: Average load – displacement curves obtained for the three composites.

In general, the CTT tensile load-displacement responses obtained show that different deformation levels are characterizing the response of each composite. Although the peak load reached in all composites was approximately the same (350 N), the displacement at which the peak load is reached was distinct, of approximately 0.5 mm in the case of the PANcc and 2 mm in the case of the PVAcc and the PPcc. The detailed analysis of the results obtained with the image-based analysis showed that cracking starts early, at tensile load values of around 150 N. When observing the measured tensile load-displacement responses of the three composites, the overall behavior and shape of the curves obtained reflect the different nature of the fiber reinforcements used. This relation will be further explored in the next section, where the influence of the composite parameters (fiber and matrix properties) on the mechanical responses obtained becomes clearer.

## SINGLE CRACK TENSION TEST (SCTT)

### 2.1 Testing procedure

The assessment of the mechanical parameters of a crack during the initiation and propagation stages requires the formation of a single crack during the entire test sequence. SHCC materials are designed to develop multiple cracks in tension, consequently the formation of a single crack is naturally prevented by the material. In a previous work [9] the dimensions and geometry presented in Figure 7 were used to consistently accomplish the formation of a single crack during testing. The length of the specimen was 120 mm and the free distance between the fixed edges during testing was 70 mm. The testing sequence consisted of applying a constant axial displacement rate of 5  $\mu\text{m/s}$  to the specimen. This deformation rate was transmitted by the hydraulic actuator by means of two hydraulic grips, providing fixed support conditions to both ends of the specimen (rotations and transverse displacements were restrained). During testing the opening of the notch was evaluated by means of two clip gages positioned in opposite sides, as shown in Figure 8.

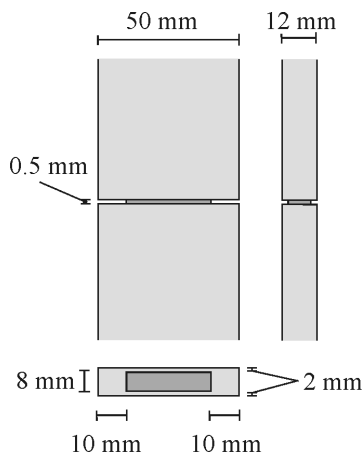


Figure 7: Geometry of the SCTT specimen.

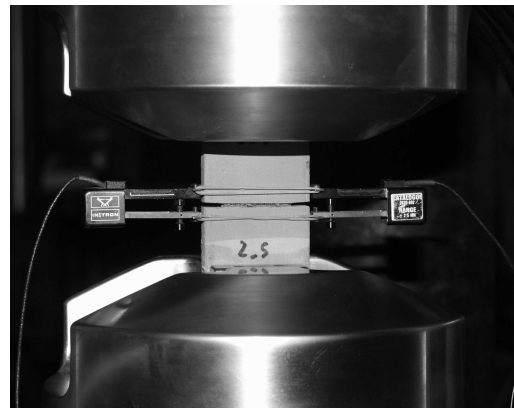


Figure 8: Tensile test-setup including supports and clip gages.

### 2.2 Tensile stress – crack opening results

The results obtained after testing six specimens of each composite in direct tension are presented in Figure 9 to Figure 12. The values of the tensile stress (nominal tensile stress) were obtained by computing the ratio between the experimental tensile load and the net area of the notched cross-section ( $8 \times 30 \text{ mm}^2$ ). The crack mouth opening displacements (CMOD) were obtained by averaging the displacements measured in the two opposite clip gages.

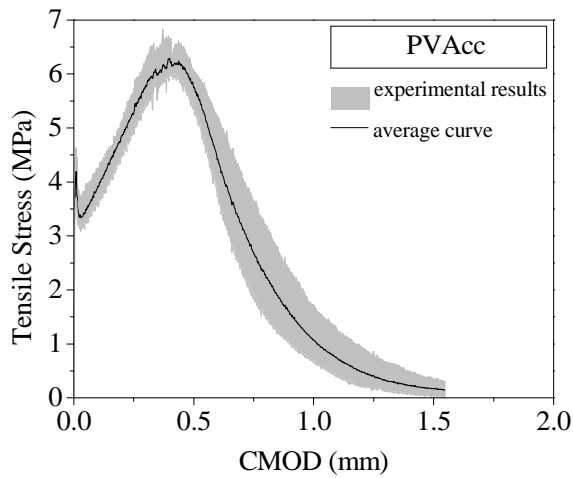


Figure 9: Tensile stress-CMOD for the composites reinforced with PVA fibers.

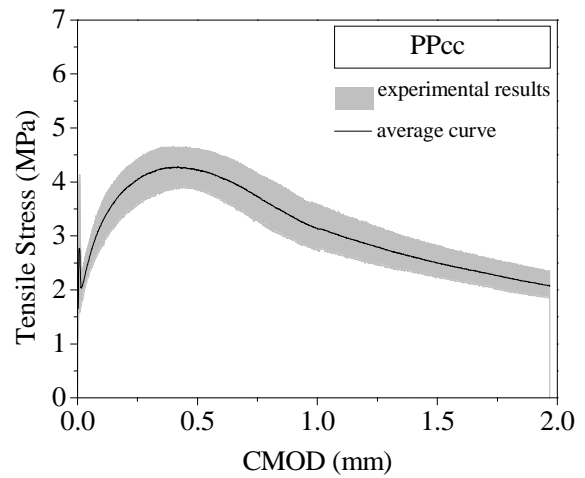


Figure 10: Tensile stress-CMOD for the composites reinforced with PP fibers.

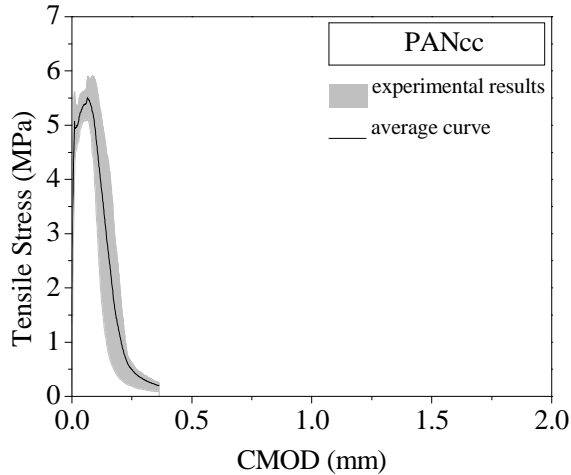


Figure 11: Tensile stress-CMOD for the composites reinforced with PAN fibers.

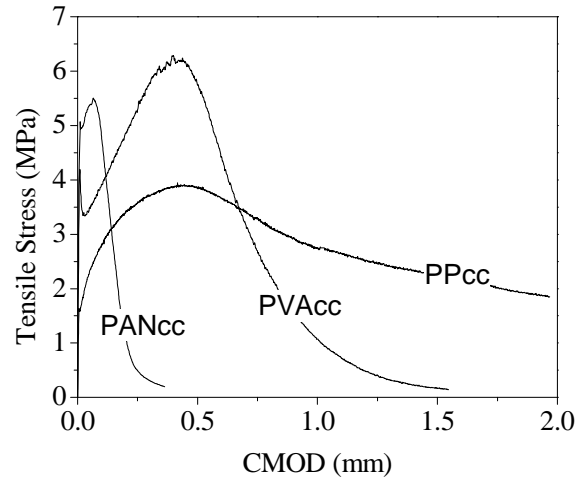


Figure 12: Average tensile stress-CMOD curves obtained for the three composites.

As shown in Figure 9 to Figure 12, the activation of fibers with different diameters and of different natures occurs at different stages of the cracking process. The PAN fibers, with a smaller diameter, were activated even before the first cracking stress was reached, and have contributed effectively to increase the cracking peak stress. Their premature effective activation was followed by an also premature exhaustion of their contribution to the post-cracking tensile behavior. The contribution of PVA and PP fibers to increase the first cracking strength was insignificant. Instead, their full mobilization became apparent in the post-cracking stage, with the pronounced increase of the tensile bridging stress. The main difference between the SCTT results observed for PVA and PP fibers locates at the region of the tensile stress-CMOD curves where the peak bridging stress is reached. While for the PVA reinforced composites the experimental curves exhibited a sharp transition from the tensile hardening to the tensile softening stage of the tensile bridging stress, for the PP reinforced composites this transition was smooth and gradual. The well known superior interfacial bonding of the PVA fibers with the matrix may justify these results, as opposed to the poorer bonding of the PP fibers due to their hydrophobic nature [18,19]. Further discussion regarding the significance of each stage of the tensile stress-CMOD responses obtained with the SCTT can be found elsewhere [9].

### 3 SIMULATION OF CTT TENSILE LOAD – DISPLACEMENT RESPONSE

The tensile responses obtained with the SCTT provide information about the composite tensile behavior when a single crack is considered. The initiation of the crack is obviously determined mostly by the geometry of the specimen and the shape of the notched section. The slender notches and the strong section reduction adopted contribute to alter locally the stress fields and increase substantially the stress intensity. Therefore, the tensile responses obtained are predominantly structural until the crack is fully formed. However, after the formation of the crack is completed and the fibers remain as the final links between the opposite faces of the open crack, it may be assumed that the measured tensile bridging stress-CMOD responses are evaluated objectively and are roughly independent of specimen geometry. Consequently, this information can be used to describe the constitutive behavior of the material in tension in terms of the tensile stress,  $\sigma_t$ , as a function of the crack width,  $\delta$ . To verify this possibility, a finite element model of the CTT was constructed.

As shown in Figure 13, the geometry of the specimen and testing boundary conditions were modeled assuming plane stress conditions. The two transverse rods transmitting the load were placed in the two circular openings presented. The model was constructed using elastic 3-node linear triangular elements. The high geometrical gradients close to the notch tip were overcome with the considerable increase of the number of elements in these regions. The blunted shape of the notch tip, with a radius of 250  $\mu\text{m}$ , was discretized with increased number of finite elements. The young modulus,  $E$ , assigned to the elements was 20 GPa and the Poisson coefficient,  $\nu$ , was 0.2. One layer of interface elements was added in the notched section between the left and the right portions of the specimen ( $x = 75 \text{ mm}$ , Figure 13). The interface elements were assigned with a traction-separation law,  $\sigma_t = f(\delta)$ , directly derived from the results obtained with the SCTT of each composite. These laws correspond to the responses shown in Figure 9 to Figure 12, when the portion of the response prior to the attainment of the first cracking stress is removed. In this case the average tensile stress-crack opening responses obtained from the SCTT of each composite were utilized (Figure 12).

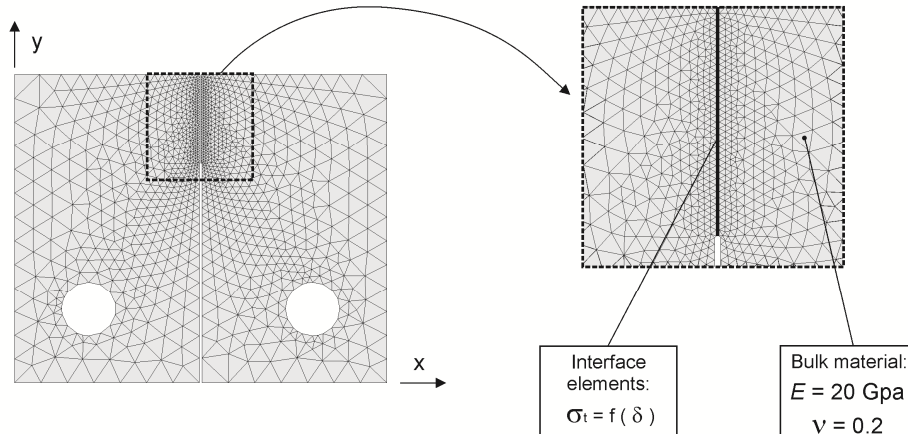


Figure 13: Tensile stress – CMOD for the composites reinforced with PAN fibers.

The tensile load-displacement responses obtained for each composite are represented in Figure 14. For each composite the computed tensile load-displacement response was compared to the experimental results (Figure 15 to Figure 17). In addition, four different stages of the CTT response obtained from one specimen for each composite were highlighted.



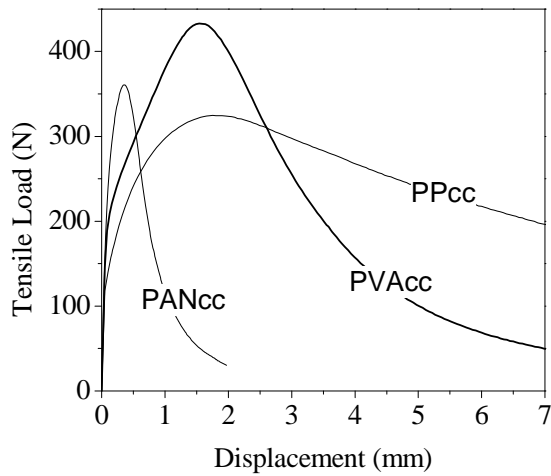


Figure 14: Tensile load – displacement response for the three composites tested.

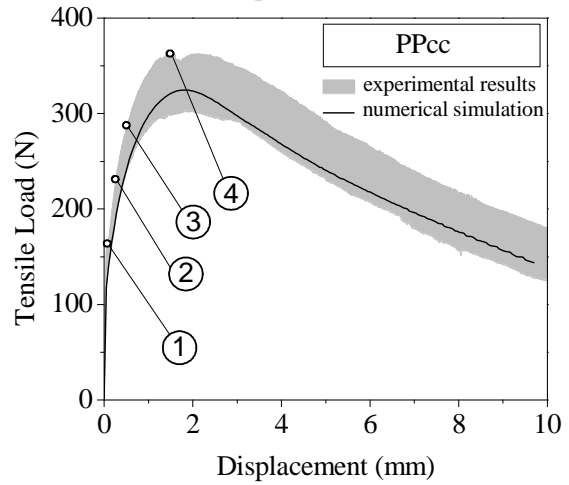


Figure 15: Tensile load – displacement response for the composites reinforced with PAN fibers.

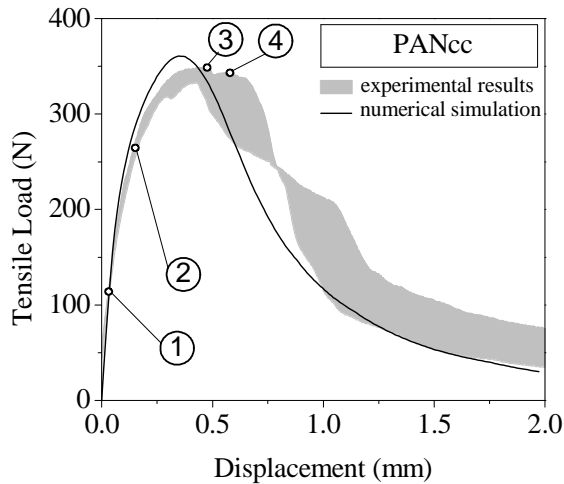


Figure 16: Tensile load – displacement response for the composites reinforced with PAN fibers.

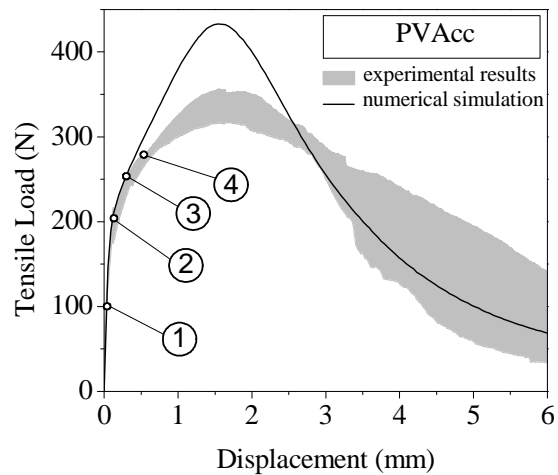


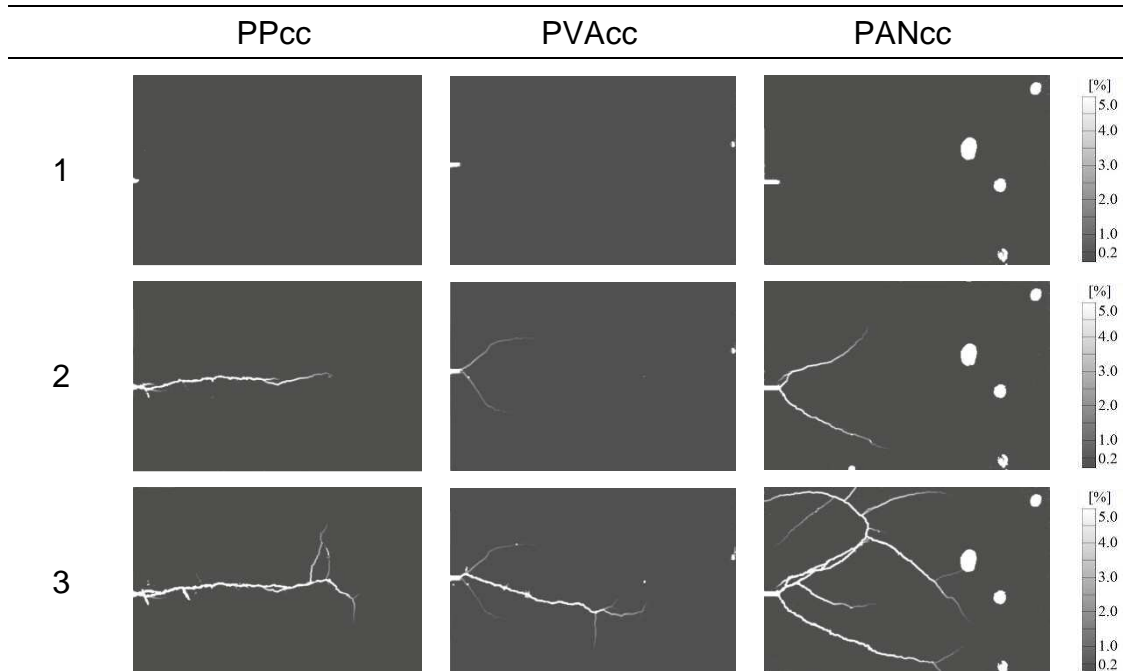
Figure 17: Tensile load – displacement response for the composites reinforced with PAN fibers.

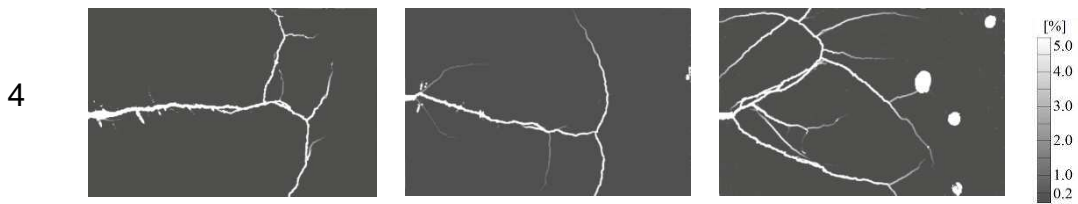
The simulated CTT responses are, in general, identical to the experimental ones. The peak load is generally overestimated by the simulations, and in contrast the displacements are generally underestimated. The formation of multiple cracks may justify this result. The finite element model assumes that a single crack is formed during the entire loading sequence, and if more than one crack is formed during testing the resulting displacements are enlarged for the same load levels. In addition, when more than one crack is formed, the rupture of the experimentally tested specimen will be eventually determined by the crack where the lowest bridging stresses are generated, among all cracks formed (the weakest link principle). The peak load overestimation is therefore the result of both the assumption of a single crack forming in the numerical model and the adoption of the average tensile stress-CMOD behavior to derive the stress-separation law of the interface elements.

The detailed analysis of the crack patterns generated at the surface of the specimens confirm that more

than one crack was formed in the tested specimens (Table 3). The stage number one was selected in all specimens to show the last stage at which no cracks were detected. All stages are identified for all specimens in Figure 15 to Figure 17. Considering the PPcc specimen, the stage two was selected as the last stage where only one major crack was detectable. Considering the PANcc and the PVAcc specimens a single major crack was never observed, at least two diagonal cracks were forming simultaneously. In the case of the PVAcc results, stages 2 and 3 are points of the tensile response where the numerical results start diverging more pronouncedly from the experimental ones. As shown in Table 3, the cracks forming in the PVAcc specimen indicate that the behavior experimentally obtained is different from the one assumed in the finite element model. The main crack diverts from its horizontal path earlier than in the other two composites, bifurcating at a considerable distance from the right border of the specimen and partly justifying the divergence between the experimental and the numerical results from stage 3 onwards. The considerable alteration of the structural behavior caused by this early crack bifurcation in the experimental test, in opposition to the assumed single crack in the numerical model, explains partly the underestimation of the experimental displacements and the overestimation of the peak tensile load by the numerical model. The profuse cracking observed in the PANcc specimen (stage 4, Table 3) also caused a substantial alteration of the structural behavior assumed in the numerical model, however the divergence between the numerical and the experimental results is not so pronounced. Although the main crack also diverts clearly from its original path, the crack branches reach longer distances in the direction of the right border of the specimen. Also, since the tensile response in the case of the PANcc is occurring at a much smaller scale, i.e., at clearly lower tensile displacements, the overestimation of the peak tensile load and the underestimation of the tensile deformation are not as pronounced as in the case of the PVAcc. In the case of the PPcc the predicted tensile response is almost identical to the experimental, and this result is supported by the observed crack pattern which is mostly identical to the one assumed by the numerical model. The displacements are, as before, somewhat underestimated by the numerical model, due to the crack branching.

Table 3: Image-based analysis of crack patterns on the surface of the specimens at stages 1 to 4.





#### 4 CONCLUSIONS

The investigation of the initiation and propagation of cracks in SHCC materials was approached in this study by performing the compact tension test (CTT) with series of specimens reinforced with different types of fibres. The tensile load-displacement responses measured have shown different characteristic tensile behaviors resulting from the different geometry and nature of the fibers used. Although the geometry of the specimen and the test setup configuration were delineated to create the necessary conditions to the initiation of a single crack, the results obtained with the image-based analysis have shown that this was not always the case. The raw pictures taken from the surface of the specimen, although with high amplifications, did not allow the detection of more than one crack. However, the post-processing of these pictures revealed disordered crack patterns substantially different from the ones assumed after a simple visual inspection. These results should be taken into account when the possibility of extracting the stress-separation law by inverse analysis is considered. The precise and explicit characterization of the stress-separation behavior by inverse analysis is only possible if the exact crack pattern formed is known in advance, and the model used to simulate the experimental response is able to accommodate these complex crack patterns.

The characterization of the tensile stress-CMOD behavior of the three different fiber reinforced cementitious composites using the single crack tension test (SCTT) has shown high sensitivity to the main parameters of each cementitious composite. The post-cracking behaviors obtained have shown that different fibers have an optimal contribution to the tensile bridging stresses at clearly distinct scale sizes of the cracking process. The tensile stress-CMOD responses obtained with the SCTT were used to predict the tensile load-displacement behaviors obtained with the CTT of the corresponding composites. In the numerical model the typical formation of a single crack in the direction of the middle notch was assumed. Although a good general agreement between the numerical and experimental results were obtained, the peak load was somehow overestimated in some cases and the deformations underestimated by the numerical model. The results obtained with the image-based analysis explain the deviation between the numerical and the experimental results by showing the formation of cracking patterns distinct from the one assumed in the numerical model.

#### ACKNOWLEDGMENTS

The authors thank the Portuguese National Science Foundation for the financial support, through grant SFRH / BD / 36515 / 2007, funded by POPH - QREN, the Social European Fund and the MCTES, and DTU-Byg for their support of the work as part of this project.

#### REFERENCES

- [1] Brandt, A.M., "Fibre reinforced cement-based (FRC) composites after over 40 years of development in building and civil engineering." *Comp Struct* **86**: 3–9 (2008).
- [2] Li, V.C., "On engineered cementitious composites (ECC) - A Review of the Material and Its Applications" *J Adv Conc Tech* **1**(3): 215-230 (2003).
- [3] Kanda, T., Li, V.C., "Practical design criteria for saturated pseudo strain hardening behavior in ECC." *J Adv Conc Tech* **4**(1):59-72 (2006).
- [4] Naaman, A.E. and Reinhardt, H.W., "Proposed classification of HPFRC composites based on their tensile response." *Mat Struct* **39**:547–555 (2006).

- [5] Shah, S.P., Swartz, S.E. and Ouyang, C., *Fracture mechanics of concrete: applications of fracture mechanics to concrete, rock, and other quasi-brittle materials*, John Wiley & Sons Inc, New York (1995).
- [6] Yang, J. and Fischer, G. "Investigation of the Fiber Bridging Stress – Crack Opening Relationship on Fiber Reinforced Cementitious Composites" In: G. Fischer G and Li VC (eds.) *High Performance Fiber Reinforced Cementitious Composites in Structural Applications: RILEM Proceedings PRO 49*, RILEM SARL, pp 93-105 (2006).
- [7] Fischer, G., Stang, H. and Dick-Nielsen, L., "Initiation and development of cracking in ECC materials: experimental observations and modeling." In Carpinteri GFA., Gambarova P (eds). *Proc. Int. Symp. Ia-FraMCos, Vol. 3*, Taylor & Francis, pp 1517–1522 (2007).
- [8] *RILEM TC TDF-162.*, "Test and design methods for steel fiber reinforced concrete. Recommendations for uniaxial tension test." *Mat Struct* **34**: 3–6 (2001).
- [9] Pereira, E.B., Fischer, G., Barros, J.A.O. and Lepech, M., "Crack formation and tensile stress-crack opening behavior of fiber reinforced cementitious composites (SHCC)." In Oh BH, Choi OC, Chung L (eds). *Proceedings of FraMCoS-7*, Jeju, Korea, May 23-28 (2010). ISBN 978-89-5708-181-5.
- [10] Hornain, H., Marchand, J., Ammouche, A., Commène, J.P. and Moranville, M., "Microscopic observation of cracks in concrete – a new sample preparation technique using dye impregnation." *Cement Concrete Res* **26**(4): 573-583 (1996).
- [11] Otsuka, K. and Date, H., 'Fracture process zone in concrete tension specimen.' *Eng Fract Mech* **65**: 111-131 (2000).
- [12] He, S., Feng, Z. and Rowlands, R.E., "Fracture Process Zone Analysis of Concrete Using Moiré Interferometry." *Exp Mech* **37**(3): 367-373 (1995).
- [13] Knab, L.I., Walker, H.N., Clifton, J.R. and Fuller, Jr. E.R., "Fluorescent thin sections to observe the fracture zone in mortar." *Cement Concrete Res* **14**: 339-344 (1984).
- [14] Shah, S.P., "Experimental methods for determining fracture process zone and fracture parameters." *Eng Fract Mech* **35**:3-14 (1990).
- [15] Chu, T.C., Ranson, W.F., Sutton, M.A., Peters, W.H., "Applications of digital-image-correlation techniques to experimental mechanics", *Exp Mech* **25**(3): 232-244 (1985).
- [16] Pereira, E.B., Fischer, G. and Barros, J.A.O., "Image-based detection and analysis of crack propagation in cementitious composites" In Leung, C.K.Y. (ed). *Proceedings of Advances in Concrete through Science and Engineering - RILEM*, Hong Kong, September 23-28 (2011).
- [17] Berfield T.A., Patel J.K., Shimmin R.G., Braun P.V., Lambros J., Sottos N.R., "Micro- and nanoscale deformation measurement of surface and internal planes via digital image correlation". *Exp. Mech.* **47**: 51-62 (2007).
- [18] Li, V.C., Wu, C., Wang, S., Ogawa, A. and Saito, T., "Interface tailoring for strain-hardening poly(vinyl alcohol – engineered cementitious composite (PVA-ECC)." *ACI Mat J* **99**(5): 463-472 (2002).
- [19] Wei, Q.F., Mather, R.R., Fotheringham, A.F. and Yang, R.D., "ESEM study of wetting of untreated and plasma treated polypropylene fibers." *J Ind Tex* **32**(1): 59-66 (2002).